04,08

Paramagnetic centers of uncontrolled impurities in $ZnWO_4$ doped with rare earths and lithium

© V.A. Vazhenin[1], M.Yu. Artyomov[1], A.P. Potapov[1], K.A. Soubbotin[2,3], A.V. Fokin[1], Yu.I. Zimina[2,3], A.I. Titov[2], D.A. Lis[2]

[1] Ural Federal University (Institute of Natural Sciences and Mathematics), Yekaterinburg, Russia
[2] Prokhorov Institute of General Physics, Russian Academy of Sciences, Moscow, Russia
[3] Mendeleev University of Chemical Technology, Moscow, Russia

E-mail: vladimir.vazhenin@urfu.ru

Received June 28, 2025
Revised July 28, 2025
Accepted August 8, 2025

Single crystals of $ZnWO_4$ grown by the Czochralski method and doped with Yb or Tm, as well as Li, were studied by the EPR method. Transitions of monoclinic centers of Fe^{3+}, Cr^{3+} and Gd^{3+} were observed, similar to the previously studied spectra in lithium-free crystals. Spectra of triclinic centers detected in samples free of lithium admixture and attributed to dimers (paramagnetic ion - zinc vacancy) were not observed. However, new satellites appeared, accompanying the transitions of monoclinic centers in a wide range of magnetic field orientations. It is reasonable to assume that these centers (triclinic and monoclinic) arise as a result of association of paramagnetic ions with lithium ions in zinc positions. Measurement of the orientational behavior of intradoublet (in the case of Gd^{3+} — and interdoublet) transitions in two orthogonal planes made it possible to determine the parameters of their spin Hamiltonians.

Keywords: zinc tungstate, impurity ions, iron group, REE, paramagnetic resonance.

DOI: 10.61011/PSS.2025.09.62351.216-25

1. Introduction

A zinc tungstate single crystal ($ZnWO_4$) is well known for a long time as an effective scintillation material [1–5], which is in particular promising as a cryogenic scintillation detector when detecting rare events [1,6]. Moreover, recently, crystals $ZnWO_4$ doped with three-charged rare-earth ions (REI, Ln^{3+}) are extensively investigated as promising laser media [7–11].

One of the most important problems of the $ZnWO_4$ crystal is abrupt degradation of its spectrum-generation and scintillation characteristics when a crystal composition is polluted even with trace quantities of accidental impurities of $3d$-ions, primarily, iron. In this case, noticeable parasitic optical absorption appears in the crystal in the wavelength range below 600 nm [3,12–14], which prevents efficient laser generation from REIs in the visible spectral range. At the same time, there is also reduction of intensity of photo-, X-ray- and cathodoluminescence [15] as well as light yield of scintillation of the crystal [16,17].

Although there is no doubt that this parasitic absorption is directly related to presence of the iron impurity in the crystal, a specific nature of this absorption is still unclear. At least, values of peak sections of this absorption ($\sim 10^{-16}\,cm^2$) make it impossible to interpret these absorption bands as belonging to usual electron-vibrational transitions inside a $3d$-shell of ions Fe^{2+} or Fe^{3+}. Moreover, introduction of some additional dopants into the crystal (Nb^{5+}, Ta^{5+}, Sb^{5+}, Ag^{+}, etc.) completely removes this spurious optic absorption [13,16], although it is obvious that iron does not disappear from the crystal when doing so. Besides, efficiency of scintillation of the crystal is not restored when introducing these additional impurities [16]. Thus, it can be assumed that the accidental impurity of iron and some other $3d$-ions forms in the $ZnWO_4$ crystal some special structures that provide absorption bands of anomalously high specific intensity, which are easily destroyed when introducing the said additional impurities. It is still relevant to investigate a structure and crystallochemical behavior of these structures.

An important problem of zinc tungstate as a laser matrix is also a fact that heterovalent substitution of relatively small double-charged ions Zn^{2+} with quite large three-charged REIs in the crystal structure without introducing additional charge compensators into its composition results in sharp degradation of mechanical strength characteristics of crystals [18,19]. At the same time, coefficients of distribution of even the smallest ones of them (Tm^{3+} and Yb^{3+}) between the crystal and a melt hardly reach 0.25 [18,19].

Basically, this problem could have been partially solved by additionally introducing ion-charge compensators (Li^{+}, Na^{+}, K^{+}, Nb^{5+}, Ta^{5+}) into the crystal [11,18–21]. However, in actual practice it turned out that Na^{+} and K^{+} only insignificantly increase the coefficients of distribution of

the REIs in the crystal $ZnWO_4$ [11,20,21], while the ions Nb^{5+} and Ta^{5+} can not be introduced into the crystal in any significant concentrations without sharp degradation of an optic quality of the crystal (cracking and formation of inclusions of secondary phases).

The best one of the charge compensators tested up to now is an ion Li^+. Introduction of this ion into the crystal structure in actual concentrations that are equimolar with the REIs made it possible to increase the coefficient of distribution of the ions Yb^{3+} in zinc tungstate up to 0.5 [18], and the ions Tm^{3+} therein up to 0.45 [19]. At the same time, the actual REI concentrations in the crystals could be brought to several at.% relative to zinc, while the mechanical strength characteristics of these crystals are not worse than for nominally-pure $ZnWO_4$ and even better than for it according to preliminary data [18,19].

However, issues and problems are also present here. The coefficient of distribution of lithium itself in the zinc tungstate crystal is less than for Yb^{3+} and Tm^{3+}. Moreover, trends toward its further decrease with an increase of the REI concentration in the crystal [18,19] are revealed, although it would seem that a mechanism of conjugate isomorphism to be switched on when jointly doping the crystal with the ions Li^+ and the REIs shall provide a reverse trend. It means in practice that for a Czochralski growth of the crystals Ln^{3+}, Li^+:$ZnWO_4$ with the equimolar actual concentrations of the REIs and lithium at a level of several at.% of each, a nominal concentration of lithium in an initial melt shall be about $20-25$ at.% relative to a total number of the ions claiming to occupy zinc positions of the crystal structure $(Zn^{2+} + Ln^{3+} + Li^+)$, while the total concentration of both the dopants in the melt even at the initial stage of the growth shall be just half the zinc concentration. As growth progresses, these concentrations become even higher. Such high concentrations of the dopants actually mean that the crystal is grown already not from the melt, but rather from a quite concentrated solution in the melt with the entire set of problems arising therefrom: from a necessity of sharp reduction of a crystallization rate to increased probability of formation of bubbles and inclusions of the secondary phases in the crystal.

Finally, lithium is an element which is not the most convenient due to a small atomic number. An arsenal of analytical methods suitable for controlling the actual concentration of lithium and its associates with rare-earth ions in solid-state samples is quite limited and usually associated to a necessity of converting an analyzed sample into a solution form. Therefore, it is relevant to optimize the concentration of lithium in melts for growing the crystals Ln, Li:$ZnWO_4$ based on refinement of mechanisms of crystallochemical processes occurring in such double doping as well as to search for other more effective charge compensators for heterovalent introduction of the REIs into the composition of the zinc tungstate crystal. It is quite problematic to purposefully solve this problem without clearly knowing actual concentrations and structures of impurity defects that occur in the crystal when introducing the REIs and the charge compensators of the various types into its composition.

A method of electron paramagnetic resonance (EPR) is quite effective for investigating structural localization of REI activators in the crystals taking into account defects that are formed during heterovalent entry of the defects (including intentionally introduced impurity defects) and compensate excess charge. Besides, the EPR is an effective method of detecting microconcentrations of accidental impurity ions with unpaired electrons in the crystals and of revealing a nature of active centers based thereon.

The present study continues a cycle of our EPR investigations of the $ZnWO_4$ crystals doped with the REIs as well as jointly doped by the REIs and various charge compensators. It should be noted that it is somewhat difficult to observe most three-charged REIs (except for the ions Gd^{3+}) by the EPR methods. Thus, their signals are observed only at cryogenic temperatures. At the same time, the ions Gd^{3+} are available for sure EPR detection even at the temperatures that significantly higher than the room one. On the other hand, these ions in microconcentrations are almost always present as a random impurity in the crystals doped with other REIs, while the crystallochemical behavior of the ions Gd^{3+} is quite similar to that for the other three-charged REIs. Therefore, in the present cycle of the studies, while being enabled with EPR observation of impurity ions of gadolinium, we consider them to be a marker that reflects presence and structural localization of the other REIs in the zinc tungstate crystals.

In the first study of the present cycle [22], we investigated the Tm:$ZnWO_4$ crystal grown by the Czochralski method in air from a platinum crucible. The actual concentration of thulium in the crystal was 0.62 at.% relative to the zinc content, while charge compensators were not introduced into the crystal composition. The study has detected and investigated monoclinic paramagnetic centers (PC) of the accidental impurities Fe^{3+}, Cr^{3+} and Gd^{3+} (hereinafter referred to as centers Fe1, Cr1 and Gd1), which substituted the ions Zn^{2+} with nonlocal compensation of excess positive charge. Moreover, the said sample demonstrated EPR spectra of additional triclinic-symmetry paramagnetic centers that are designated as Fe2, Fe3, Cr2, Cr3 and Gd2, Gd3 and assumed to originate as a result of appearance of a zinc vacancy that reduces PC symmetry in the nearest surrounding of the respective paramagnetic ion. We have determined parameters of spin Hamiltonians (SH) of all the said centers. A ratio of concentrations of triclinic and monoclinic centers of iron, chromium and gadolinium has been estimated.

In this paper, we continue the study initiated in the paper [22]. Several samples of the zinc tungstate single crystals codoped with the ions Tm/Li and Yb/Li are studied within its framework. A role of lithium as the charge compensator during REI entry into the crystal was estimated.

2. Samples and experimental procedure

Within the framework of the present paper, the EPR studies were performed with taken samples of the $ZnWO_4$ crystals grown by the Czochralski method within the framework of the papers [18] and [19] with the following (charge) concentrations of the dopants: No. 1: 5 at.% Yb + 5 at.% Li, No. 2: 4 at.% Yb + 16 at.% Li and No. 3: 7 at.% Tm + 24 at.% Li. The actual concentrations of the dopants in these crystals relative to zinc were: the sample No. 1: 2.0 at.% Yb + 1.5 at.% Li; the sample No. 2: 2.7 at.% Yb + 2.5 at.% Li; the sample No 3: 3.7 at.% Tm + 1.9 at.% Li. Charge synthesis, growth and annealing of the crystals, measurement of the actual concentrations of the dopant as well as refinement of orientation of the crystals relative to optical indicatrix axes are described in the studies [18,19].

The studied samples were manufactured as rectangular parallelepipeds with polished facets that were orthogonal to the optical indicatrix axes (hereinafter referred to as the planes N_g, N_m, N_p). A relation between crystallographic axes and the optical indicatrix axes for nominally-pure $ZnWO_4$ is shown in the studies [7,8].

A space group of $ZnWO_4$ is P2/c (C_{2h}^4) No. 13, and lattice cell parameters $\mathbf{a} = 4.69$ Å, $\mathbf{b} = 5.72$ Å, $\mathbf{c} = 4.92$ Å, $\beta = 90.6^\circ$ [23]. Both cations in the crystal are surrounded by six oxygen ions that form monoclinically distorted octahedrons, and a local symmetry group of the positions of Zn^{2+} and W^{6+} is $2(C_2)$.

Orientation behavior of the positions of the EPR transitions was measured when rotating a magnetic field within the plane $\mathbf{a}-\mathbf{c}$ and within the plane $\perp N_g$ on an X-band spectrometer EMX Plus Bruker at the room temperature in the magnetic fields of up to 1.4 T. The parameters of the spin Hamiltonians were determined both in the laboratory system of coordinates XYZ ($Z \parallel N_m$, $Y \parallel N_p \equiv \mathbf{b}$) and in the local (principal) system of coordinates xyz Cr1 (z is rotated from the axis $+\mathbf{a}$ to $+\mathbf{c}$ by 4.2°). It is in this system of coordinates that the parameters of the triclinic centers Fe2, Fe3, Cr2, Cr3, Gd2, Gd3 are given in the study [22].

The sample in a spectrometer resonator was fixed to one end of a quartz tube attached to a standard automatic goniometer. The crystal was initially set in a microwave resonator (the plane $N_m \perp B$, where B is induction of the magnetic field) by observing a laser beam reflected from the polished facet of the sample through a standard window of the resonator.

3. Results and discussion

Accurate setting of orientation of the sample facets relative to a direction of the magnetic field and measurement of an angular dependence of the positions of the EPR signals within the plane $\mathbf{a}-\mathbf{c}$ made it possible to determine an angle between the principal axis z of the monoclinic center Cr1 [22] and the axis N_m. For the $ZnWO_4$ sample No. 2 this angle turned out to be $+10^\circ$, for the sample No. 3 $+11^\circ$, and for the sample No. 1 — 5°. For the crystal investigated by us in the paper [22] and doped only by thulium with the actual concentration of 0.6 at.% relative to zinc (hereinafter referred to as the sample No. 0), this angle is $+12^\circ$. An error of determination of all the said angles is $\pm 1^\circ$. An average value of the angle for the samples Nos. 0, 2 and 3 is about $+11^\circ$.

Thus, the sample No. 1 clearly stands out of the said series. In our opinion, it is related to the fact that this sample in relation to the optical indicatrix axes was erroneously oriented. Due to an error in orientation of the facet of the sample No. 1, the behavior of the spectrum thereon was measured in a plane perpendicular to the direction (hereinafter referred to as N) that is spaced from N_g within the plane $\mathbf{a}-\mathbf{c}$ by $\sim 16^\circ$.

According to results of the studies [7,8,24], the angle between the axis N_m and the principal axis z of the monoclinic center Cr1 for the lightly-doped $ZnWO_4$ is $+15.9^\circ$. An issue of how crystal doping affects the value of this angle is currently investigated by us. We plan to publish a separate paper on results of this investigation.

Figure 1 shows the EPR spectra in orientation $B \parallel Y \parallel \mathbf{b}$ of the two $ZnWO_4$ REI-doped samples. As expected, the crystal codoped with thulium and lithium exhibits signals of the same accidental impurities — Fe^{3+} and Gd^{3+}, as for the previously studied crystal No. 0 doped only with thulium. At the same time, however, it is well clear that an increase of a concentration of the thulium impurity as well as introduction of lithium results in an increase of the line width and, therefore, degradation of resolution. A low-field wing of the transition Fe1 (177 mT) of the highly-doped sample No. 3 originated intense signals that were absent in the spectrum of the crystal No. 0. Besides, the signals of the paramagnetic centers Cr1, Cr2, Cr3 and Mn^{2+} have almost disappeared in the sample No. 3 [22], although in the other studied samples (No. 1 and 2) the weak spectrum of Cr1 is still observed. Taking into account that the samples No. 0 and 3 were grown using the same batches of initial reagents ZnO, WO_3 and Tm_2O_3, this fact can be explained either by entry of microimpurities Cr and Mn into the melt and, whence, the sample No. 0 from process equipment when growing or preparing the charge, or by too strong broadening and, therefore, a decrease of peak intensity of the respective lines, as a result of which these signals cease to be resolved against the background of stronger signals of iron and gadolinium.

In the three lithium-containing samples (the samples Nos. 1–3), the measured angular dependences of the positions of the EPR transitions of the monoclinic centers Fe1 (the electron spin $S = 5/2$), Cr1 ($S = 3/2$) and Gd1 ($S = 7/2$) are satisfactorily described by the SH parameters given in the study [22] for the sample No. 0 (lithium-free) (Figure 2). Similar values of the SH parameters were also obtained by the authors [24–28] for the $ZnWO_4$ samples doped with iron, chromium or gadolinium. In addition to the monoclinic chromium center (Cr1), the study [27] also

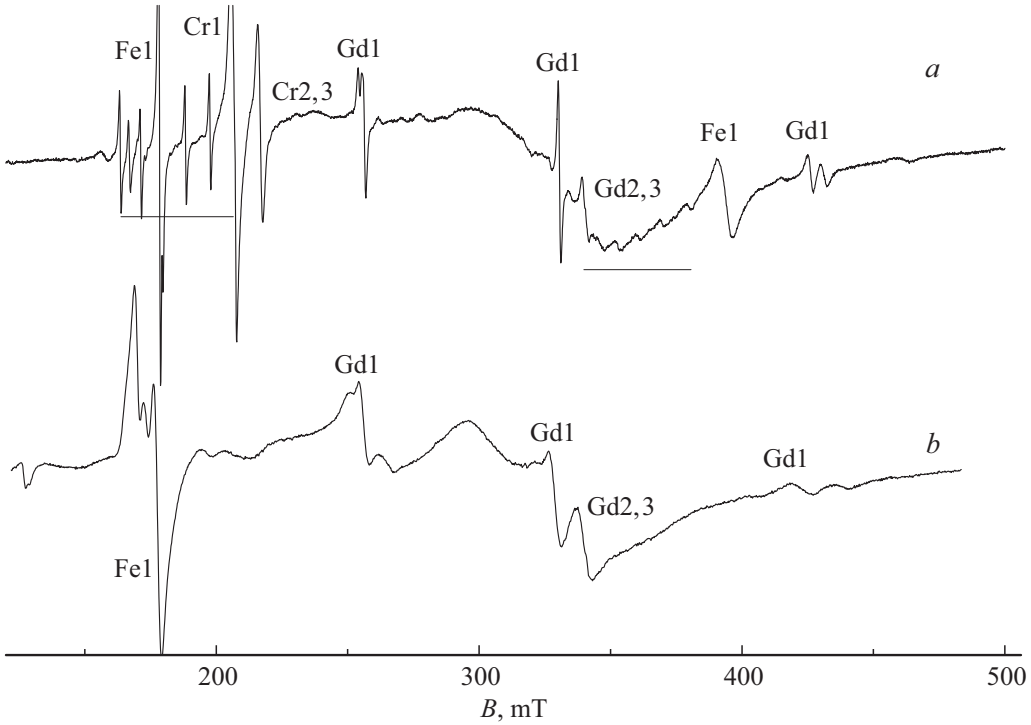

Figure 1. Fragments of the EPR spectra (the first derivative of the absorption spectrum) when B || Y || **b**. *a* — the sample No. 0 at the frequency of 9608 MHz [22], *b* — the sample No. 3 at the frequency of 9570 MHz. Horizontal line fragments show ranges of fields of two hyperfine-structure sextets of the center of Mn^{2+}.

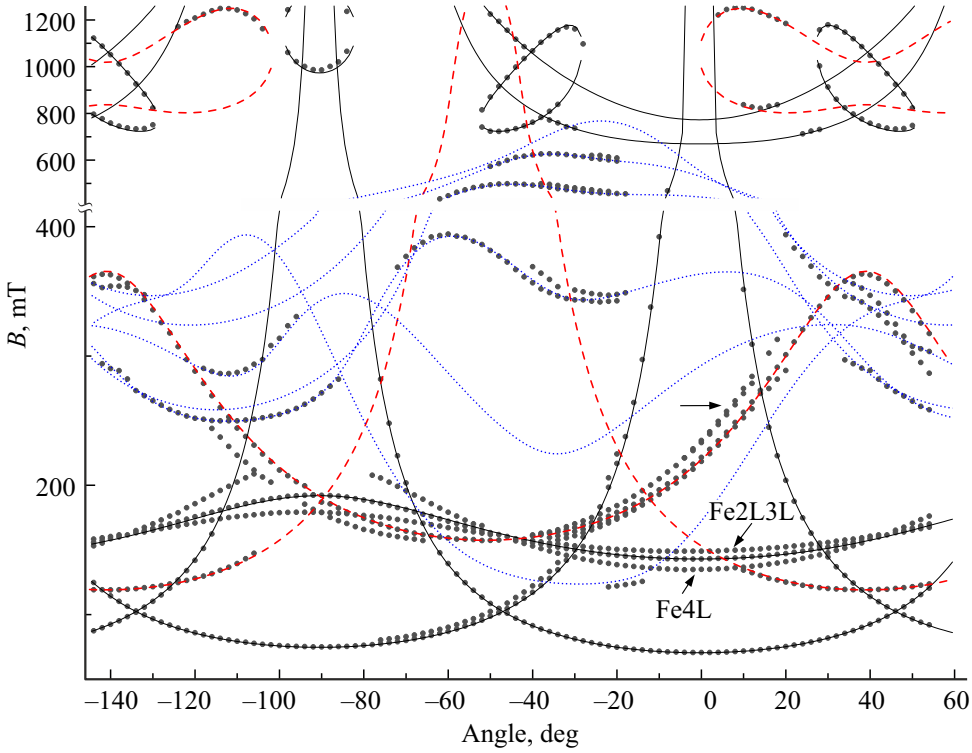

Figure 2. Orientation behavior of the positions of the EPR signals of the sample No. 1 when rotating the magnetic field within the plane **a**−**c** at the frequency of 9728 MHz. A zero of the abscissa axis corresponds to z(Fe1). The dots denote an experiment, the black solid curves denote a calculation for Fe1, the red dashed curves denote a calculation for Cr1, and the blue dotted curves denote a calculation for Gd1 with the parameters [22]. The horizontal arrow indicates transitions 1−2 of the centers Cr2L and Cr3L.

detected in the chromium-doped zinc tungstate low-intensity EPR spectra of two pairs of the triclinic centers of Cr^{3+} (Cr2, Cr3 and Cr4, Cr5) that are pairwise connected by an operation C_2. The authors of the study assumed that the said centers corresponded to the $Cr^{3+}-V_{Zn}$ associates. Absence of interdoublet transitions in the spectrum [27] made it difficult to estimate a value of zero magnetic field splitting (ZFS).

It is clear in Figure 2 that in addition to the transitions of the said monoclinic centers there are also signals of new centers. Let us designate as Fe2L, Fe3L, Cr2L and Cr3L. These signals with the orientation behavior close to the transitions of the centers Fe1 and Cr1 are similar to vanished resonances of the triclinic centers Fe2, Fe3, Cr2 and Cr3, which are described in the study [22] and seem to correspond to associates of chromium and iron with zinc vacancies. However, here field distances from the signals of the monoclinic centers are different from those for impurity-vacancy associates (Figure 2). We believe that the signals of Fe2L, Fe3L, Cr2L and Cr3L correspond to associates of the ions Fe^{3+} and Cr^{3+} with lithium ions in the zinc position.

In addition, we have managed to detect additional satellites (in particular, a monoclinic paramagnetic center that is designated by us as Fe4L and shown in Figure 2), which also demonstrate the angular dependence close to the transitions of the main monoclinic centers.

The signals of the triclinic centers Gd2 and Gd3, which are shown in Figure 8 of the study [22] and seem to be related to the $Gd^{3+}-V_{Zn}$ associates, are absent in the lithium-containing samples, but weak satellites appear on the wings of the Gd1 transitions, which are visible in Figure 2 within a narrow range of the angles near $-30°$. Most likely, these signals are induced by dimers $Gd-Li_{Zn}$ with a large distance to the lithium ion (Li is not in the nearest Zn position). A more accurate conclusion requires a theoretical model on a relation of the SH parameters to the dimer distances.

Thus, doping the samples Nos. 1–3 with lithium resulted in disappearance (or reduction of intensity below a sensitivity limit of the spectrometer) of the signals of the paramagnetic dimers that are associated with V_{Zn} and in origination of a noticeable number of the dimers, seemingly, with involvement of the ions Li_{Zn}. It is very difficult to quantitatively evaluate the concentrations of these centers at such a low content of the paramagnetic impurities.

The spectra of pairs of the centers Fe2L and Fe3L (Cr2L and Cr3L) and in the same way as Fe2 and Fe3 (Cr2 and Cr3) within the plane **a**–**c** of all the samples are equivalent, while within the plane perpendicular to the axis N_g their signals are noticeably split, coinciding when B ∥ Y ∥ **b** (Figures 3, 4). Unlike the orientation behavior of the spectrum of the sample No. 2 (Figure 5), at the angles above 5° the sample No. 1 (Figure 2) exhibits slight splitting of the transition 1–2 (1, 2 are numbers of the energy levels) of the centers Cr2L and Cr3L (marked by the horizontal arrow). This splitting is explained by deviation of the magnetic field from the plane **a**–**c** (in our estimates, by a value of about 1°). An additional series of dots below

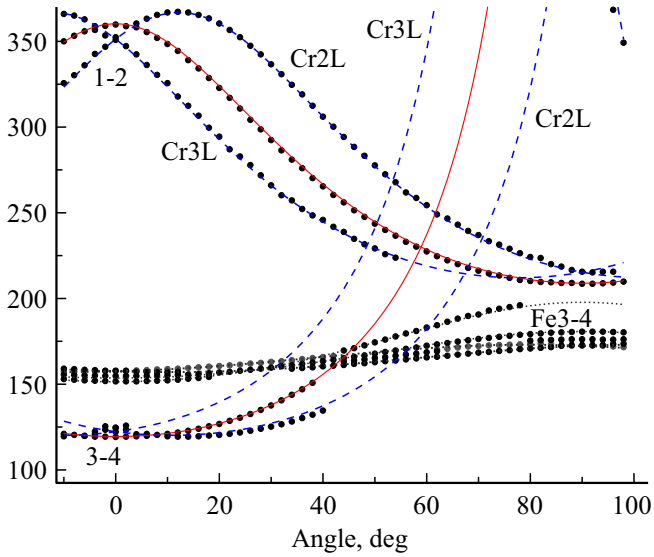

Figure 3. Angular dependence of the positions of the two interdoublet transitions of the centers Cr2L, Cr3L and Cr1 of the sample No. 1 within the plane ⊥N, at the frequency of 9727 MHz. The dots denote an experiment, the red solid curves denote a calculation for the centers Cr1, the blue dashed curves denote a calculation for Cr2L, Cr3L, and the black dotted curves denote a calculation for the transitions Fe^{3+}.

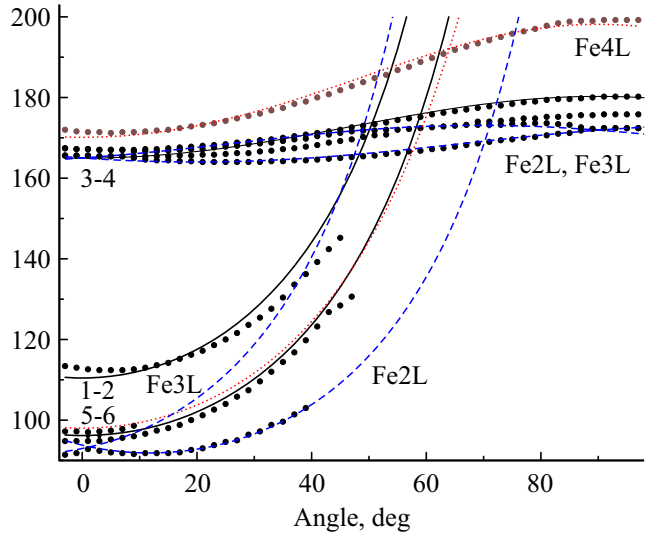

Figure 4. Angular dependence of the positions of the three interdoublet transitions of the centers Fe2L, Fe3L and Fe1 of the sample No. 3 within the plane ⊥ N_g at the frequency of 9703 MHz. The dots denote an experiment, the black solid curve denotes a calculation for the centers Fe1, the blue dashed curves denote a calculation for Fe2L, Fe3L, and the red dotted curves denote a calculation for Fe4L.

the signals of the center Cr1 in this angle range is induced by existence of yet another dimer center, whose parameters could not be determined due to a lack of experimental data.

Unlike the centers Fe2L, Fe3L and Fe2, Fe3, a satellite of the transition 3–4 Fe1 (Fe4L, in Figures 3, 4 at 90° its

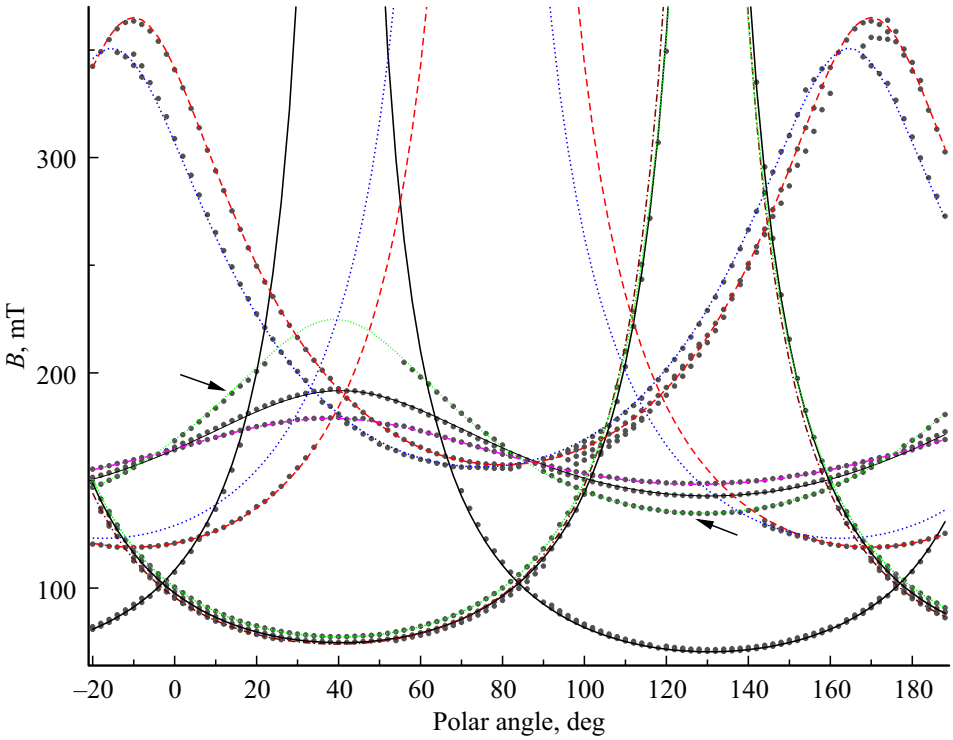

Figure 5. Orientation behavior of the positions of the EPR signals of the sample No. 2 when rotating the magnetic field within the plane **a**−**c** at the frequency of 9715 MHz. The angles are counted along the abscissa axis from the optical indicatrix axis N_m. The dots denote an experiment, the black solid curves denote a calculation for Fe1, the red dashed curves denote a calculation for Cr1, the blue short dashed curves denote a calculation for Cr2L, the purple dash-dotted curve denotes a calculation for Fe2L, and the green dashed curves denote a calculation for Fe4L with the parameters of Tables 1−3. The arrows indicate an angular dependence of the position of the transition 3−4 of the center Fe4L.

position is ~ 200 mT) is not split in this plane. The other interdoublet transitions (5−6 and 1−2) of this paramagnetic center are most likely hidden in the wings of the signals of Fe1. Within the plane **a**−**c**, the positions of the transition 3−4 of the center Fe4L, (they are marked by the arrows in Figure 5) do not demonstrate splitting as well. Figure 4 also exhibits yet another satellite of the signal of Fe1, which is not split in this plane (at 90° the position is ~ 176 mT), whose positions within the plane **a**−**c** could not be measured.

Parameters of the triclinic spin Hamiltonian [29] of the centers Cr2L, Cr3L in the three samples were optimized by a least-square method using positions of the transitions in the two planes. Using a set of parameters of the centers Cr1 [22] as an initial one, we have obtained results shown in Table 1.

It is clear from Table 1 that in the single system of coordinates with z(Cr1) [22] the sets of the SH parameters, which well describe the experimental dependences (Figure 5), as well as the ZFS values noticeable differ for the various studied samples, although we are talking about the same paramagnetic center. It is due to the fact that the used experimental material has not positions of the interdoublet transitions, which are directly related to the ZFS value. The parameters of the monoclinic center Cr1 ($b_{20} = 25490$ MHz, $b_{22} = -7230$ MHz, ZFS ≈ 51 GHz [22]), as well as the triclinic centers Cr2, Cr3 ($b_{20} = 22000$ MHz, $b_{22} = -12100$ MHz, ZFS ≈ 59 GHz [22]) in the system of coordinates of the center Cr1 are most closely matched with the values of b_{2m} and the ZFS value, which are obtained for the centers Cr2L, Cr3L in the sample No. 1 (Table 1). In the principal system of coordinates, this center has the monoclinic SH with $b_{20} = 27880$ MHz, $b_{22} = 8620$ MHz and Euler angles $\alpha = 245.7°$, $\beta = 13.3°$, $\gamma = 205.3°$.

The similar procedure of optimization for the paramagnetic centers Fe2L, Fe3L and Fe4L led to the results shown in Tables 2, 3. As in the case of the paramagnetic centers Cr2L, Cr3L, the sets of the parameters of the triclinic centers Fe2L, Fe3L and the monoclinic center Fe4L in the single system of coordinates noticeable differ from one sample to another. The interdoublet transitions could not be recorded for these centers as well. Thus, the SH parameters that are shown in Tables 2, 3 and satisfactorily describe the experiment in the three samples can not claim to be characteristic values of an energy structure of the listed paramagnetic centers.

Zero field splitting of the monoclinic centers Cr1 and Fe1 is approximately equal to 51 GHz and $61 + 77 = 138$ GHz, respectively [24,25]. These values are quite close to the

Table 1. SH parameters of the centers Cr2L, Cr3L (the double signs c_{21} and c_{22}) in the three $ZnWO_4$ samples and in the two systems of coordinates when Y $\|$ **b**. F is a mean-square error, n is a number of used positions of the signals. ZFS is zero magnetic field splitting

Samples	No. 1		No. 3		No. 2	
Parameters	Z $\perp$ N	z(Cr1)	Z$\|\|$ N_m	z(Cr1)	Z$\|\|$ N_m	z(Cr1)
g	1.96					
b_{20}, MHz	26220	25800	15460	17780	16930	19270
b_{21}, MHz	−1790	−17210	−34690	−13080	−37310	−15900
b_{22}, MHz	−10280	−9860	−4550	−6870	−5230	−7570
c_{21}, MHz	±30840	±30720	±18290	±19620	±23780	±25890
c_{22}, MHz	0	∓1340	∓4380	∓2555	∓7130	∓4960
ZFS, GHz	≈ 56		≈ 40		≈ 45	
F(n), MHz	28(183)		40(123)		47(177)	

Table 2. SH parameters of the centers Fe2L, Fe3L (the double signs c_{21} and c_{22}) in the three $ZnWO_4$ samples and in the two systems of coordinates when Y $\|$ **b**. F(n), b_{nm} and c_{nm} in MHz, ZFS in GHz. The ZFS line for Fe^{3+} (S = 5/2) includes a sum of the two interdoublet intervals

Samples	No. 3		No. 1		No. 2	
Parameters	Z $\|\|$ N_m	z(Cr1)	Z$\perp$ N	z(Cr1)	Z$\|\|$ N_m	z(Cr1)
g	2.002					
b_{20}	3810	−5010	−7020	−3700	2995	−6000
b_{21}	90290	91300	74310	77200	102220	101880
b_{22}	−8810	14	2120	−1190	−8060	940
b_{40}	120	100	0	0	280	240
b_{41}	0	300	0	−20	0	780
b_{42}	0	480	0	−140	0	615
b_{43}	−4665	−4175	−3150	−3080	−5940	−5400
b_{44}	0	−430	0	140	0	−500
c_{21}	±18980	±19290	±15140	±15460	±19310	±19940
c_{22}	∓1720	±122	±2170	±1500	∓2670	∓950
ZFS	≈ 164(74 + 90)		≈ 140(64 + 76)		≈ 191(92 + 99)	
F(n)	23 (251)		15 (181)		16 (212)	

Table 3. SH parameters of the centers Fe4L in the three $ZnWO_4$ and in the two systems of coordinates when Y $\|$ **b**. F(n) and b_{nm} in MHz, ZFS in GHz

Samples	No. 3		No. 1		No. 2	
Parameters	Z $\|\|$ N_m	z(Cr1)	Z$\perp$ N	z(Cr1)	Z$\|\|$ N_m	z(Cr1)
g	2.002					
b_{20}	1570	−4900	−11690	−8310	540	−4790
b_{21}	66200	66910	74655	79850	60550	60280
b_{22}	−10060	−3590	1390	−1990	−8260	−2930
b_{40}	−770	−790	−685	−705	−370	−400
b_{41}	1810	−1520	−1160	260	1160	−430
b_{42}	180	460	810	680	175	510
b_{43}	−3020	−1710	−3940	−4580	−3170	−2010
b_{44}	−550	−1090	−590	−400	−860	−1090
ZFS	≈ 123(53 + 70)		149(62 + 87)		≈ 109(44 + 65)	
F(n)	35 (197)		15 (107)		26 (206)	

Table 4. Ratio of the concentrations of the monoclinic and triclinic centers of Fe^{3+} and Cr^{3+} in the three crystals of doped zinc tungstate

No. of the sample	Measured concentrations of the dopants	Ratio of the concentrations	
		c(Fe2L + Fe3L)/cFe1	c(Cr2L + Cr3L)/cCr1
1	2.0 at.% Yb + 1.5 at.% Li	0.016	0.12
2	2.7 at.% Yb + 2.5 at.% Li	0.04	0.17
3	3.7 at.% Tm + 1.9 at.% Li	0.06	0.11

ZFS values shown in Tables 1–3 for the dimer centers Cr2L, Cr3L, Fe2L, Fe3L and Fe4L. Proximity of their energy structure is also indicated by the fact that the dimer transitions usually accompany signals of single paramagnetic centers. Accordingly, the interdoublet transitions of the dimer paramagnetic centers shall occur approximately in the same fields, in which similar signals for the centers Cr1 and Fe1 are detected. Absence of these transitions in our measurements is most likely due to a low concentration of uncontrolled impurities of chromium and iron in the samples and an even lower (by more than an order, see below) number of the dimer centers. Further progress in investigation of the dimer centers in $ZnWO_4$ requires measurements of samples that are specially doped with ions of iron, chromium or gadolinium in concentrations which radically higher those in the samples investigated in the present study. We plan these actions for the next stage of our work.

Integral intensities of the EPR signals were evaluated by using spectra in a magnetic field orientation that corresponds to the angle (-74°) in Figure 2. Strong overlapping of the transitions of the monoclinic centers Fe1 and Cr1 and the triclinic centers did not allow correct double integration of the observed signals. Therefore, the integral intensity was assumed to be a product of peak intensity of the first derivative by a square of the width of the line ΔB_{pp}. Taking into account calculated probabilities of the observed transitions resulted in values of the concentration ratios, which are shown in Table 4. Signals of the satellites Gd1 turned out to be too weak for analysis, especially in the sample No. 2.

The dimer triclinic centers Cr2, Cr3, Fe2, Fe3 [22] and Cr2L, Cr3L, Fe2L, Fe3L are pairwise equivalent only at the magnetic field in the plane **a**–**c** and when B ∥ **b**. It is possible when the compensator V_{Zn} (or Li_{Zn}) in the dimer is localized in a neighboring (below or above the position of the paramagnetic ion) layer of the Zn ions, which is perpendicular to the axis **b**. The crystal symmetry operation C_2 generates the second dimer center with an alternative direction of the bond axis, while there is no limitation on the direction of the bond axis of the dimer in the plane **a**–**c**.

Unlike the above-listed paramagnetic centers, the spectrum of the center Fe4L does not demonstrate splitting of the EPR signals in the studied planes and, therefore, it is monoclinic. This behavior shall be expected in dimer associates, whose bond axis is parallel to **b** or lies in the plane **a**–**c**. In this case, two equivalent dimers with antiparallel bond axes are realized. Resolving an issue of localization of charge-compensating defects requires involvement of a microscopic theory that takes into account a binding energy of the dimers in question.

As for the ratio of the concentrations of the monoclinic paramagnetic centers that correspond to the ions Fe^{3+} and Cr^{3+} with nonlocal charge compensation, which are included in the crystal structure in a heterovalent way, and the triclinic paramagnetic centers with lithium ions localized in direct proximity to the paramagnetic ion, it is clear from Table 4 that the centers with nonlocal charge compensation obviously prevail, whose content is by 1–2 orders higher than that of the iron-lithium and chromium-lithium associates. This numbers indicate that in the $ZnWO_4$ crystals a mechanism contributing to dimer self-organization of the ions Fe^{3+} (Cr^{3+}) and the ions Li^+ is not highly efficient, but still present in a certain degree.

4. Conclusion

We discuss a problem of producing the high-quality $ZnWO_4$ crystals as the laser matrix in conditions when it is necessary to substitute relatively small double-charged zinc ions with large three-charged REIs. The optical properties of the crystals depend both on a type of defects that compensate the REI excess charge as well as the microscopic concentrations of the uncontrolled 3*d* ions. Information about a structure of the accidental impurities and their interaction with the charge compensators was obtained by using the EPR method.

The $ZnWO_4$ single crystals with the actual concentrations of the dopants (2.0 at.% Yb + 1.5 at.% Li); (2.7 at.% Yb + 2.5 at.% Li); (3.7 at.% Tm + 1.9 at.% Li), which were grown by the Czochralski method, were studied in the X-band EPR spectrometer. The spectra of the monoclinic centers Cr1, Fe1 and Gd1 with nonlocal charge compensation in the said samples practically did not differ from the spectra in the crystal No. 0 that is doped with 0.6 at.% Tm and does not contain lithium [22].

The signals of the triclinic paramagnetic centers Cr2, Cr3, Fe2, Fe3 that are believed to be locally compensated due to closely-located zinc vacancies have disappeared, but some new signals (Cr2L, Cr3L, Fe2L, Fe3L, Fe4L) with another field distance from the transitions of the respective monoclinic centers have appeared. The spectrum

of the triclinic centers Gd2 and Gd3 was not observed, whereas the weak satellites appear on the wings of the Gd1 transitions. It is logical to assume that all the said satellites of the transitions of the centers Cr1, Fe1 and Gd1 are respective transitions in the dimer complexes with involvement of Li_{Zn}.

Using the orientation behavior of the positions of the interdoublet transitions of the paramagnetic centers Cr2L, Cr3L, Fe2L, Fe3L and Fe4L in the optimization procedure, the parameters of their spin Hamiltonians have been obtained. The respective SH parameters in the three samples (Tables 1–3) differ due to uncertainties in calculations, which are related to absence of the interdoublet transitions in the spectrum, which provide information about the ZFS value.

It is shown that the mechanism contributing to self-organization of the ions $Fe^{3+}(Cr^{3+})$ and Li^+ into the dimer centers in the zinc tungstate crystal is not highly efficient: a predominant number of the ions Fe^{3+} and Cr^{3+} in the studied crystals has nonlocal charge compensation, i.e. the nearest lithium ion is spaced quite far from the ion $Fe^{3+}(Cr^{3+})$ so as not to noticeably affect local symmetry of the paramagnetic center.

Funding

The study was financially supported by the Ministry of Science and Higher Education of the Russian Federation, topic No. FEUZ-2023-0017 using the equipment provided by Ural Common Use Center „Modern Nanotechnologies“ of Ural Federal University (Reg. No. 2968).

Conflict of interest

The authors declare that they have no conflict of interest.

References

[1] V.B. Mikhailik, H. Kraus. J. Phys. D: Appl. Phys. **39**, 1181 (2006).
[2] V. Nagirnyi, E. Feldbach, L. Jonsson, M. Kirm, A. Kotlov, A. Lushchik, V.A. Nefedov, B.I. Zadneprovski. Nuclear Instruments and Methods in Physics Research A **486**, 395 (2002).
[3] L.L. Nagornaya, A.M. Dubovik, Y.Y. Vostretsov, B.V. Grinyov, F.A. Danevich, K.A. Katrunov, V.M. Mokina, G.M. Onishchenko, D.V. Poda, N.G. Starzhinskiy, I.A. Tupitsyna. IEEE Trans. Nucl. Sci. **55** (3), 1469 (2008).
[4] D.M. Trots, A. Senyshyn, L. Vasylechko, R. Niewa, T. Vad, V.B. Mikhailik, H. Kraus. J. Phys.: Cond. Matter **21**, 1 (2009).
[5] A. Dubovik, Yu.Yu. Vostretsov, B. Grinberg, F. Danevich, H. Kraus. Acta Physica Polonica A **117**, 1 (2010).
[6] M. Buryi, V.V. Laguta, Jirí Hybler, M. Nikl. Physica Status Solidi B **248**, 993 (2011).
[7] A. Volokitina, S.P. David, P. Loiko, K. Subbotin, A. Titov, D. Lis, R.M. Sole, V. Jambunathan, A. Lucianetti, T. Mocek, P. Camy, W. Chen, U. Griebner, V. Petrov, M. Aguilo, F. Díaz, X. Mateos. Journal of Luminescence **231**, 117811 (2021).
[8] G.Z. Elabedine, K. Subbotin, P. Loiko, Z. Pan, K. Eremeev, Y. Zimina, Y. Didenko, S. Pavlov, A. Titov, E. Dunina, L. Fomicheva, A. Kornienko, A. Braud, R.M. Solé, M. Aguiló, F. Díaz, W. Chen, P. Volkov, V. Petrov, X. Mateos. Opt. Materials **157** (1), 116039 (2024).
[9] Z. Xia, F. Yang, L. Qiao, F. Yan. Optics Communications **387**, 357 (2017).
[10] F.G. Yang, Z.Y. You, C.Y. Tu. Laser Phys. Lett. **9** (3), 204 (2012).
[11] F.G. Yang. J. Materials Research, **27** (16), 2096 (2012).
[12] X. Leng, D. Li, C. Xu, Y. Xu, X. Jin. Optik **125**, 1267 (2014).
[13] A. Watterich, O.R. Gilliam, L.A. Kappers. Solid State Commun. **88**, 619 (1993).
[14] A. Kornylo, A. Jankowska-Frydel, B. Kuklinski, M. Grinberg, N. Krutiak, Z. Moroz, M. Pashkowsky. Radiat. Meas. **38**, 707 (2004).
[15] K. Subbotin, A. Titov, V. Solomatina, A. Khomyakov, E. Pakina, V. Yakovlev, D. Valiev, M. Zykova, K. Kuleshova, Y. Didenko, D. Lis, M. Grishechkin, S. Batygov, S. Kuznetsov, I. Avetissov. Materials **16**, 2611 (2023).
[16] X. Leng, D. Li, C. Xu, Y. Xu, X. Jin. Optik **125**, 1267 (2014).
[17] L.N. Limarenko, Y.V. Zorenko, M.M. Batenchuk, Z.T. Moroz, M.V. Pashkovskii, I.V. Konstankevich. J. Appl. Spectrosc. **67** (2), 287 (2000).
[18] K.A. Subbotin, A.I. Titov, S.K. Pavlov, P.A. Volkov, V.V. Sanina, D.A. Lis, O.N. Lis, Y.I. Zimina, Y.S. Didenko, E.V. Zharikov. J. Crystal Growth **582**, 126498 (2022).
[19] Yu.I. Zimina, K.A. Subbotin, A.I. Titov, P.A. Volkov, Ya.S. Didenko, D.A. Lis, S.K. Pavlov, E.V. Zharikov. Physics of Wave Phenomena, **33**, *3*, 227 (2025).
[20] F. Yang, C. Tu, J. Li, G. Jia, H. Wang, Y. Wei, Z. You, Z. Zhu, Y. Wang, X. Lu. Optical Materials **157**, *9*, 116039 (2024).
[21] F. Yang, C. Tu. The spectroscopy investigation of $ZnWO_4$:Tm^{3+} single crystal. J. Alloys and Compounds, **535**, 83 (2012).
[22] V.A. Vazhenin, A.P. Potapov, K.A. Subbotin, M.Yu. Artemov, Yu.I. Zimina, A.V. Fokin, A.I. Titov, D.A. Lis, P.A. Volkov. FTT **67**, 478 (2025). (in Russian).
[23] W.S. Brower Jr., P.H. Fang. J. Appl. Phys. **41**, 2266 (1970).
[24] S.K. Kurtz, W.G. Nilsen. Phys. Rev. **128**, 1586 (1962).
[25] W.G. Nilsen, S.K. Kurtz. Phys. Rev. **136**, A262 (1964).
[26] E.N. Emel'yanova, N.V. Karlov, A.A. Manenkov, V.A. Milyaev, A.M. Prokhorov, S.P. Smirnov, A.V. Shirkov. ZhETF **44**, 868 (1963). (in Russian).
[27] V.A. Atsarkin, L.P. Litovkina, M.L. Meil'man. FTT **7**, 3099 (1965). (in Russian).
[28] A.A. Ryadun, E.N. Galashov, V.A. Nadolinnyi, V.N. Shlegel'. Zhurnal strukturnoi chimii **53**, 696 (2012). (in Russian).
[29] S.A. Al'tshuler, B.M. Kozyrev. Elektronnyi paramagnitnyi rezonans soedinenii elementov promezhutochnykh grupp. Nauka, M. (1972). S. 121. (in Russian).

Translated by M.Shevelev